PAPER

Numerical-experimental analysis of a carbon-phenolic composite via plasma jet ablation test

Materials Research Express

PAPER

Numerical-experimental analysis of a carbon-phenolic composite via plasma jet ablation test

RECEIVED
9 March 2018

REVISED
3 May 2018

ACCEPTED FOR PUBLICATION
18 May 2018

PUBLISHED
1 June 2018

Pedro Guilherme Silva Pesci[1,2,6], **Humberto Araújo Machado**[2,3], **Homero de Paula e Silva**[2,4], **Cristian Cley Paterniani Rita**[5], **Gilberto Petraconi Filho**[5] and **Edson Cocchieri Botelho**[1]

[1] Universidade Estadual Paulista 'Julio de Mesquita Filho'–Campus Guaratinguetá; Av. Dr Ariberto Pereira da Cunha, 333-Pedregulho, Guaratinguetá-SP, Brazil, 12516-410
[2] Instituto de Aeronáutica e Espaço–IAE; Pr. Mal. Eduardo Gomes, 50, Vila das Acácias, São José dos Campos–SP, Brazil, 12228-904
[3] Universidade do Estado do Rio de Janeiro–Faculdade de Tecnologia; Rodovia Presidente Dutra, Km 298, Pólo Industrial, Resende–RJ, Brazil, 27537-000
[4] Faculdade de Engenharia Química–UNICAMP, Av. Albert Einstein, 500–Campinas–SP, Brazil, 13083-852
[5] Centro de Ciência e Tecnologia de Plasmas e Materiais, Instituto Tecnológico da Aeronáutica–ITA, Pr. Mal. Eduardo Gomes, 50, Vila das Acácias, São José dos Campos–SP, Brazil, 12228-900
[6] Author to whom any correspondence should beaddressed

E-mail: pedropesci@gmail.com

Keywords: ablation, plasma, ablative composites, thermal protection systems, reentry

Abstract

Materials used in space vehicles components are subjected to thermally aggressive environments when exposed to atmospheric reentry. In order to protect the payload and the vehicle itself, ablative composites are employed as TPS (Thermal Protection System). The development of TPS materials generally go through phases of obtaining, atmospheric reentry tests and comparison with a mathematical model. The state of the art presents some reentry tests in a subsonic or supersonic arc-jet facility, and a complex type of mathematical model, which normally requires large computational cost. This work presents a reliable method for estimate the performance of ablative composites, combining empirical and experimental data. Tests of composite materials used in thermal protection systems through exposure to a plasma jet are performed, where the heat fluxes emulate those present in atmospheric reentry of space vehicles components. The carbon/phenolic material samples have been performed in the hypersonic plasma tunnel of Plasma and Process Laboratory, available in Aeronautics Institute of Technology (ITA), by a plasma torch with a 50 kW DC power source. The plasma tunnel parameters were optimized to reproduce the conditions close to the critical re-entry point of the space vehicles payloads developed by the Aeronautics and Space Institute (IAE). The specimens in study were developed and manufactured in Brazil. Mass loss and specific mass loss rates of the samples and the back surface temperatures, as a function of the exposure time to the thermal flow, were determined. A computational simulation based in a two-front ablation model was performed, in order to compare the tests and the simulation results. The results allowed to estimate the ablative behavior of the tested material and to validate the theoretical model used in the computational simulation for its use in geometries close to the thermal protection systems used in the Brazilian space and suborbital vehicles.

1. Introduction

Space and sub-orbital vehicles reach high velocities during atmospheric reentry, resulting in aerodynamic heating. The air temperature in these cases can easily exceed 2000 °C at the stagnation point of the aircraft, which causes accelerated ablative degradation on the material. Thus, the application of a Thermal Protection System (TPS) is a must, in order to prevent damage on the payloads and astronauts. The performance of TPS materials depends on the environmental conditions of its use: heat flux intensity, chemical characteristics of the

atmosphere and boundary conditions, among other aspects. These systems are based on the principle that the energy transmitted by the heat flux through the boundary layer must be absorbed or rejected. One of the most common systems used in space vehicles TPS is the one made of ablative materials.

Ablation is a process involving surface radiation, phase change and chemical reactions. Part of the incoming heat flux is blocked by the outcoming flow of hot gases, which result from the degradation of the material. The ablative system is generally used in vehicles designed for only one mission [1–3]. The degradation of an ablative material must be an endothermic reaction such as: fusion, sublimation and carbonization, based on the principle of thermal energy absorption, yielding a fair amount of gases, resulting in thermal insulation and also in material consumption, which occurs progressively. In composite materials, ablation by carbonization is characterized by the formation of a porous char skeleton where the gases can flow through as the degradation reaction evolves, absorbing energy and blocking the heat flow when injected into the boundary layer [3–6].

Most ablative matrices are made of polymers, taking advantage of the highly endothermic nature of their degradation under non-oxidative atmospheres, as well as other good properties, such as high specific heat, low thermal conductivity and low density. Likewise, phenolic resins are used in materials in the aerospace industry due to their desirable characteristics such as high mechanical strength, heat resistance, dimensional stability, high resistance against several solvents, acids and water, flame resistance, low emission of smoke when the material is incinerated, excellent ablative properties and low cost. They absorb energy while degrading themselves, besides serving as a binder for the other components [3, 7, 8].

Charring ablators are the most commonly used thermal protection shields and are mostly produced with phenolic, epoxy or silicon resins using short fibers, silica, glass or organic spheres as reinforcement. The carbon fibers are one of the most common reinforcement types, usually obtained from cellulose fiber (Rayon), polyacrylonitrile (PAN), or tar. The process of obtaining the carbon fibers from rayon is basically carried out in three stages: stabilization or decomposition at low temperature, carbonization and graphitization [3].

TPS materials development generally go through phases of obtaining, atmospheric reentry tests and comparison with a type of mathematical model [9–11]. The present work uses simpler materials composed of carbon fiber and phenolic resin, tested in an arc-jet plasma facility aiming to validate an already developed but not yet validated simulation model of TPS design.

The numerical codes available for ablation simulation demand a vast number of chemistry and physical parameters in order to represent the process accurately, which results in a large computational cost and, in most cases, expensive campaigns of experimental tests [12].

In this work, computational simulations and experiments are combined in order to obtain a reliable method for estimate the performance of ablative composites. Some ablative properties of the composite are extracted straight from the experimental data and used to validate the empirical results, through a mathematical model developed by Machado [13] using some lumped parameters in the place of all parameters needed for the high fidelity models, which allows predicting TPS carbon/phenolic material behavior in a real geometry, under the tested heat fluxes. The model is fully described in the previous Machado's work.

The plasma arc torches are devices that convert electrical energy to thermal energy by an electric discharge between two electrodes and injecting the working gases through it, hence generating a stabile plasma jet with high flux. These devices are able to produce and maintain a directed flow with high heat flux temperatures above 3000 K, representing one of the most realistic types of simulations of the reentry conditions of space vehicles [14–16].

2. Methods

Samples made of Rayon carbon fiber and Resol phenolic matrix were taken from a rigid thermal protection blank of the Brazilian space vehicle S40 motor envelope. This kind of TPS has been used since the development of Brazilian space vehicles Sonda IV, VS-40 and VLS (Satellite Launcher Vehicle).

The carbon fiber used was a Rayon UVIS T-22 R ECHO type carbon fabric, with width of 550 $\pm$ 50 mm, thickness of 0.45 mm, weaving pattern 2 $\times$ 2 Twill, areal weight of 350 $\pm$ 35 g m^{-2} and specific mass of 1.55 g cm^{-3}. The resin matrix is a resol-type phenolic, with viscosity of 0.2 to 0.5 Pa.s at 25 °C. The impregnation process was carried out in the Plastflow company facilities, which produced the prepreg with a resin mass content of approximately 45%.

The fabrics were cut into 'petals' and arranged in a disk-shaped metal mold, lagging the seams during the stacking of the layers. The material is polymerized by the hot compression molding process, using a hydraulic press with 200 tons capacity, which has two platforms heated by electrical resistances. The curing cycle consists of a sequence of 2 h at 100 °C, 2 h at 120 °C, 2 h at 140 °C and 30 h at 165 °C, under a pressure of approximately 7 MPa. When removed from the mold, the material is as shown in figure 1(a), with 38.5 mm thickness. The

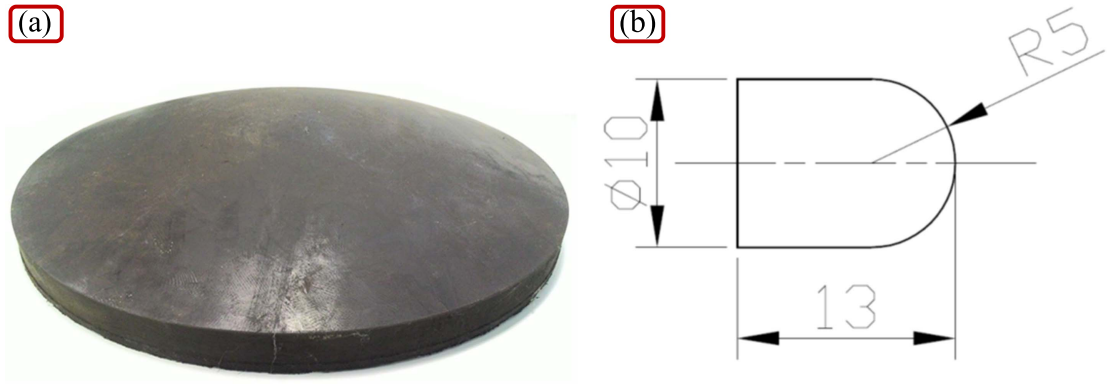

Figure 1. (a) Blank of S40 rigid thermal protection; (b) Samples geometry in [mm].

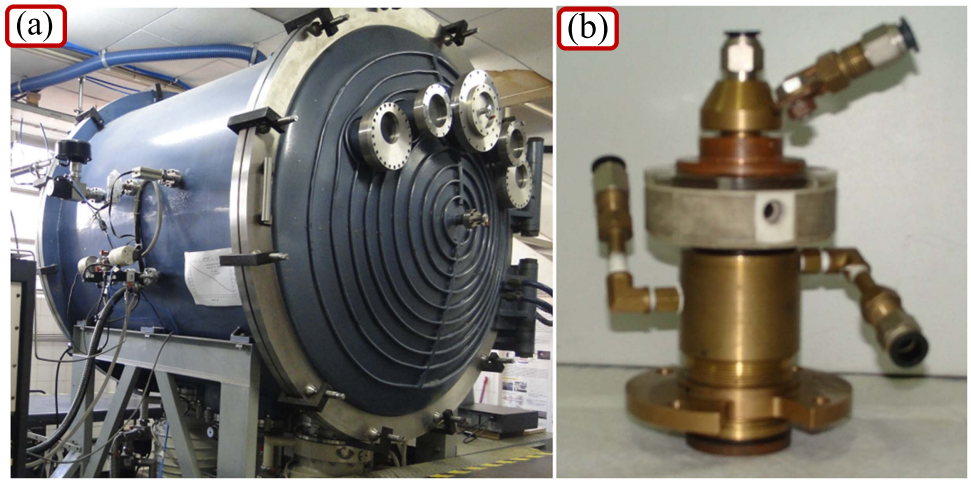

Figure 2. (a) Arc plasma facility; (b) Plasma torch.

specific mass is between 1.4 and 1.5 g cm^{-3}, its resin content in mass is between 35% and 40% and the uncured material content is less than 0.5%.

The samples were machined in the Mechanics Department of IAE, according to figure 1(b). Each sample was identified and weighed before and after the ablation tests to determine the mass loss rate. The geometry was defined based on the dimensions of the experimental apparatus, aiming a spherical surface at one end.

The ablation tests were performed in the plasma wind tunnel of the Center of Science and Technology of Plasmas and Materials (figure 2(a)). The plasma torch used in this work is a linear type with self-stabilized non-transferred electric arc (figure 2(b)), using as the working gas compressed air at 190 L min^{-1}. The assembly is coupled to a vacuum chamber (tunnel) by adaptation in one of the inspection windows of the rear chamber door [17].

The vacuum chamber has a 3.2 m^3 volume, built in stainless steel. It has a cylindrical shape of 1.5 m diameter and 1.8 m, equipped with flanges for insertion of accessories such as thermocouples, water hoses and electrical cables. A rotating structure, internally to the vacuum chamber, has eight sample holders, according to figure 3(c). These sample holders are cooled whereas the sample is fixed at the tip of the arm, as shown in figure 3(d). The arms can be rotated in order to guarantee the sample position onto the plasma jet, with the aid of a laser system.

The chamber's vacuum system is composed of a set of vacuum pumps, pressure sensors and pneumatic valves, ensuring that the pressure inside the chamber is low enough to simulate the atmospheric reentry environment (approximately 60 Pa, aiming to simulate altitudes above 50 km).

The power source provides direct current to the plasma torch, with an output voltage in open circuit of 700 V, and it is composed by six voltage transformers and one rectifier unit whit power diodes. The current can be adjusted between 25 and 120 A.

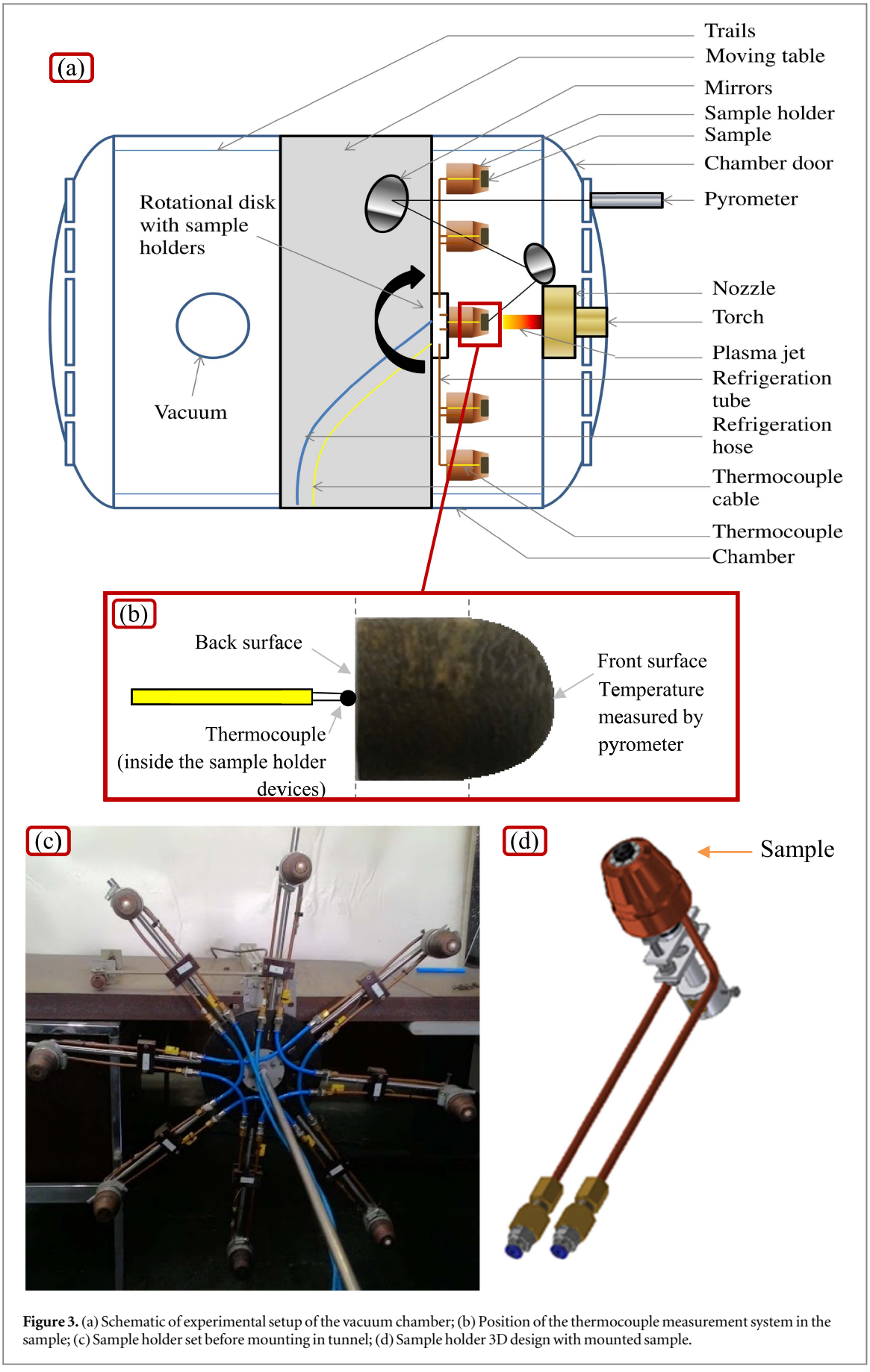

Figure 3. (a) Schematic of experimental setup of the vacuum chamber; (b) Position of the thermocouple measurement system in the sample; (c) Sample holder set before mounting in tunnel; (d) Sample holder 3D design with mounted sample.

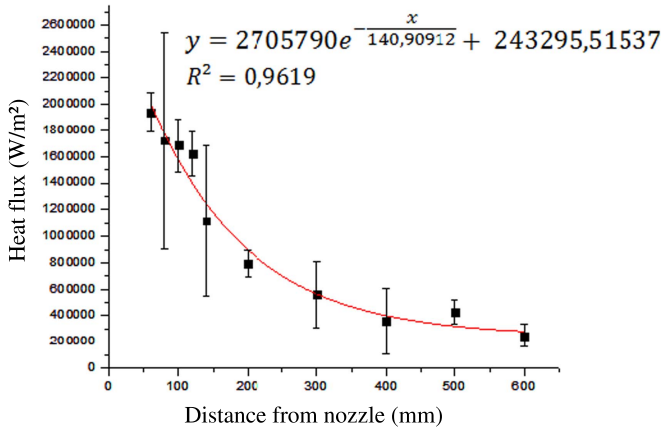

Figure 4. Thermal flux relationship with distance curve.

The heat flux of the plasma jet was measured at several distances from the nozzle, to determine a relationship between the thermal flux and the distance. A copper disk with 3 mm thickness was used as a calorimeter, which was connected to a thermocouple. The heat flux measurements were carried out as a function of time at the distances of 60, 80, 100, 120, 160, 180, 200, 300, 400, 500 and 600 mm from the nozzle (figure 4).

The samples were exposed to the plasma jet heat fluxes of 0.636, 0.903 and 1.376 MW m^{-2} at 30, 50, 70 and 90 s.

The decision on the ablation simulation model was made upon the most desirable characteristics among the following requirements:

- Accuracy: it is necessary to evaluate the deviation of the results in each case, and to determine if their use is plausible, and adequately represents the phenomenon;
- Reliability: engineering models are made up of equations that represent physical phenomena.
- Easy application: it is necessary to keep the model in a level of complexity that allows its solution with low cost.
- Flexibility of application in numerical solvers: it is desirable that in engineering models the results are obtained without the use of very expensive mathematical resources, such as coordinate transformation, mesh generation, among others;
- Working conditions and technical requirements of the IAE.

To fulfill these requirements, the mathematic model developed by Machado [13] was used. It is remarkable that this method can combine enough accuracy with the need of few parameters for calculation.

For comparison between the experimental data and the simulation, the selected parameter was the specific mass loss rate, evaluated instantaneously by the model from the integration in each step of time. Also, the temperatures and the interfaces evolution were calculated and compared to the measured ones. The model used properties taken from literature, in table 1.

3. Results

The back side temperature of the samples measured on the ablation tests was compared with those obtained by the mathematical model, as show on figure 5. After the tests, the mass loss results and their respective uncertainties enabled the construction of the curves showed on figures 6 and 7. The uncertainties were obtained by an Ohaus Precision Plus TP 4KD balance (±0.07 g), when the masses were measured and the mass loss calculated.

The specific mass loss rate ($\dot{m}$) of the samples tested in the plasma jet was obtained using the Expression 2.1, where the mass loss value in the test is divided by the projected area and the time of exposure to the plasma jet.

$$\dot{m} = \frac{(\Delta m/\pi r^2)}{t_{ej}} \tag{3.1}$$

Table 1. Carbon/phenolic properties used on the mathematical model [18–20].

Material	Property	Value
Virgin Material	Specific heat	1197 J kg^{-1} °C
	Thermal conductivity	0.867 W m^{-1} °C
	Specific mass	1398 kg m^{-3}
	Pyrolysis heat	0.465 MJ kg^{-1}
	Pyrolysis temperature	450 °C
	Emissivity	0.78
Char	Specific heat	1587 J kg^{-1} °C
	Thermal conductivity	1.58 W m^{-1} °C
	Specific mass	1135 kg m^{-3}
	Sublimation temperature	1666 °C
	Ablation heat (char)	20.88 MJ kg^{-1}
	Emissivity	0.70

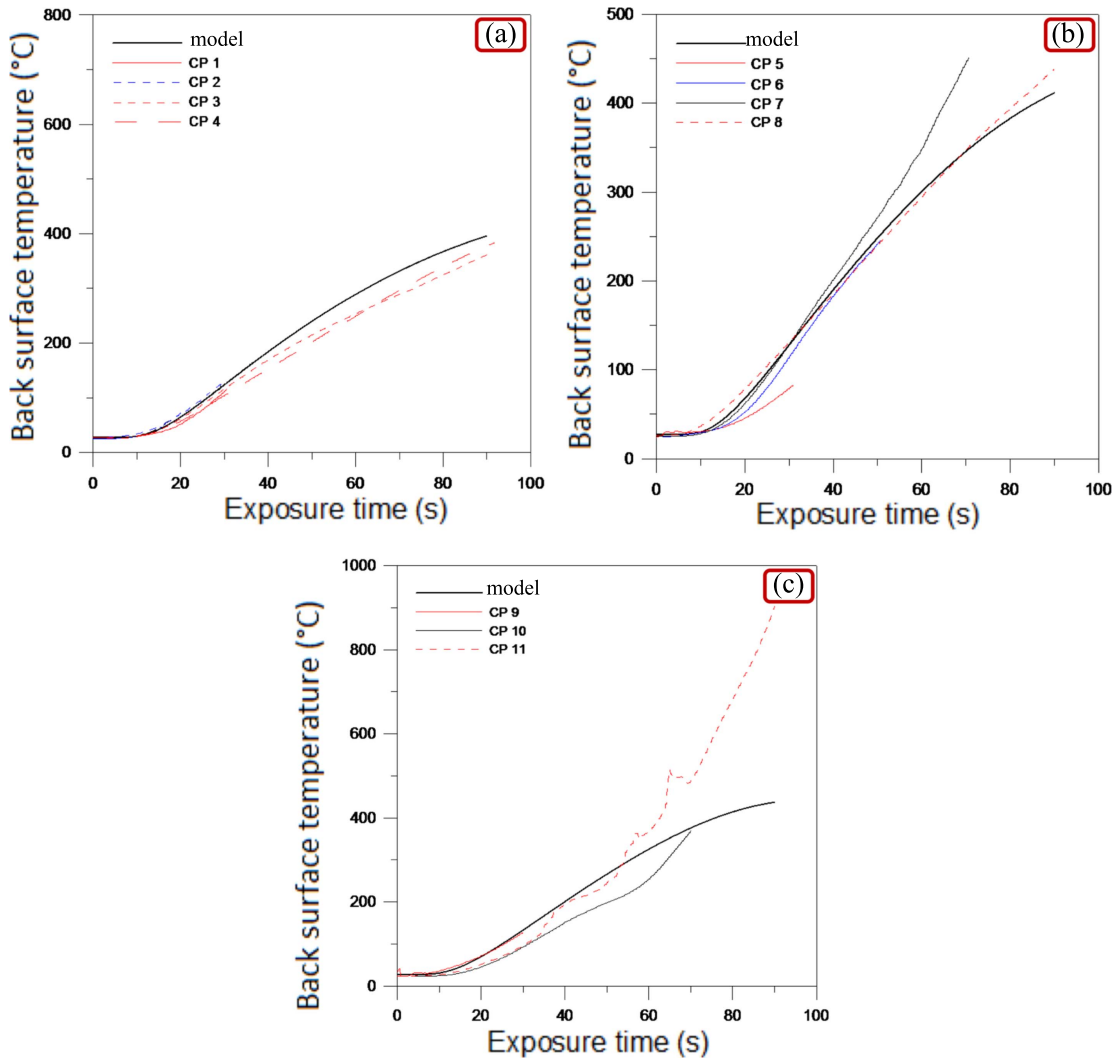

Figure 5. Simulation and experimental values of the back side temperature of the sample at: (a) 0.626 MW m^{-2}; (b) 0.903 MW m^{-2} and (c) 1.379 MW m^{-2}.

The uncertainty of the specific mass loss rate is expressed by equation (3.2):

$$\sigma_{\dot{m}} = \sqrt{\left(\frac{1}{t^2\pi^2r^4}\sigma_m^2 + \frac{4\Delta m^2}{t^2\pi^2r^6}\sigma_r^2 + \frac{\Delta m^2}{t^4\pi^2r^4}\sigma_t^2\right)} \tag{3.2}$$

These values are shown on figure 7, to each exposure time in each heat flux.

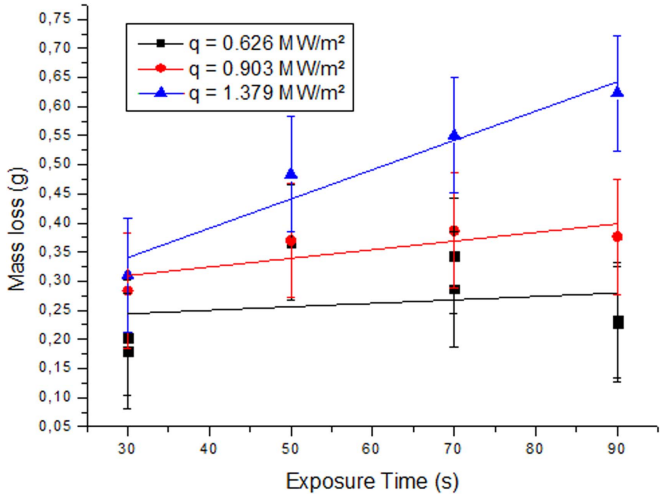

Figure 6. Mass loss curves as a function of exposure time of the tests in 0.626, 0.903 and 1.379 MW m^{-2}.

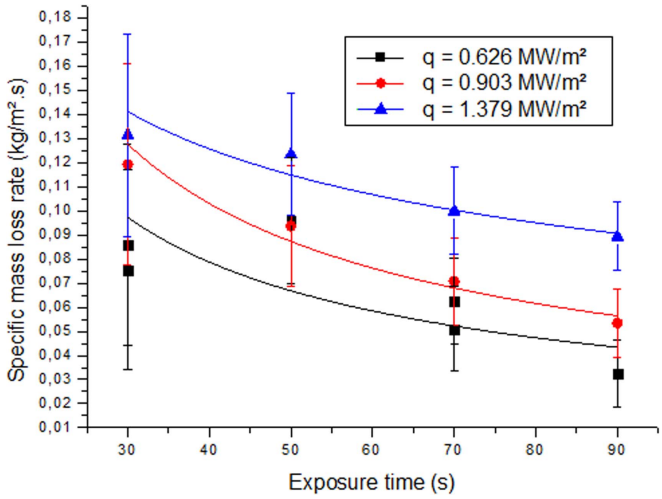

Figure 7. Specific mass loss rate curves as a function of exposure time of the tests in 0.626, 0.903 and 1.379 MW m^{-2}.

After the tests, comparisons were made between the results and the mathematical model obtaining the curves shown in figure 8:

With the mathematical model, it was possible to predict the interfaces evolution of char ablation (red) and pyrolysis (blue). The results are shown on figure 9. These results were compared to the real interfaces evolution of the experimental results. Figure 10 shows three examples.

4. Discussions

It is possible to verify, in figure 5, that the simulation curve remained in all cases in the average of the temperatures. In figure 5(a), the curves remained with a similar behavior the one found by the model. Figure 5(b) shows a closer result to the model curve. In figure 5(c), the results remained close to the simulation until the time of 70 s, when the curve of the sample (CP) 11 starts to show different. This non-linear behaviors measured by the thermocouple are justified by turbulence generated by the experimental apparatus, which contains quartz/phenolic parts that suffers ablation after a bunch of experiments, generating volatiles which influence the measurements of the test.

Figures 6 and 7 show that mass loss grows with the exposure time while the specific mass loss rate shows a reduction with the exposure time to the plasma jet. At the beginning of the process there was only virgin material. With exposure to heat flow, the char formation begins. Although its thermal conductivity is greater than the virgin material's, the reduction of specific mass loss rate over time shows that the formation and

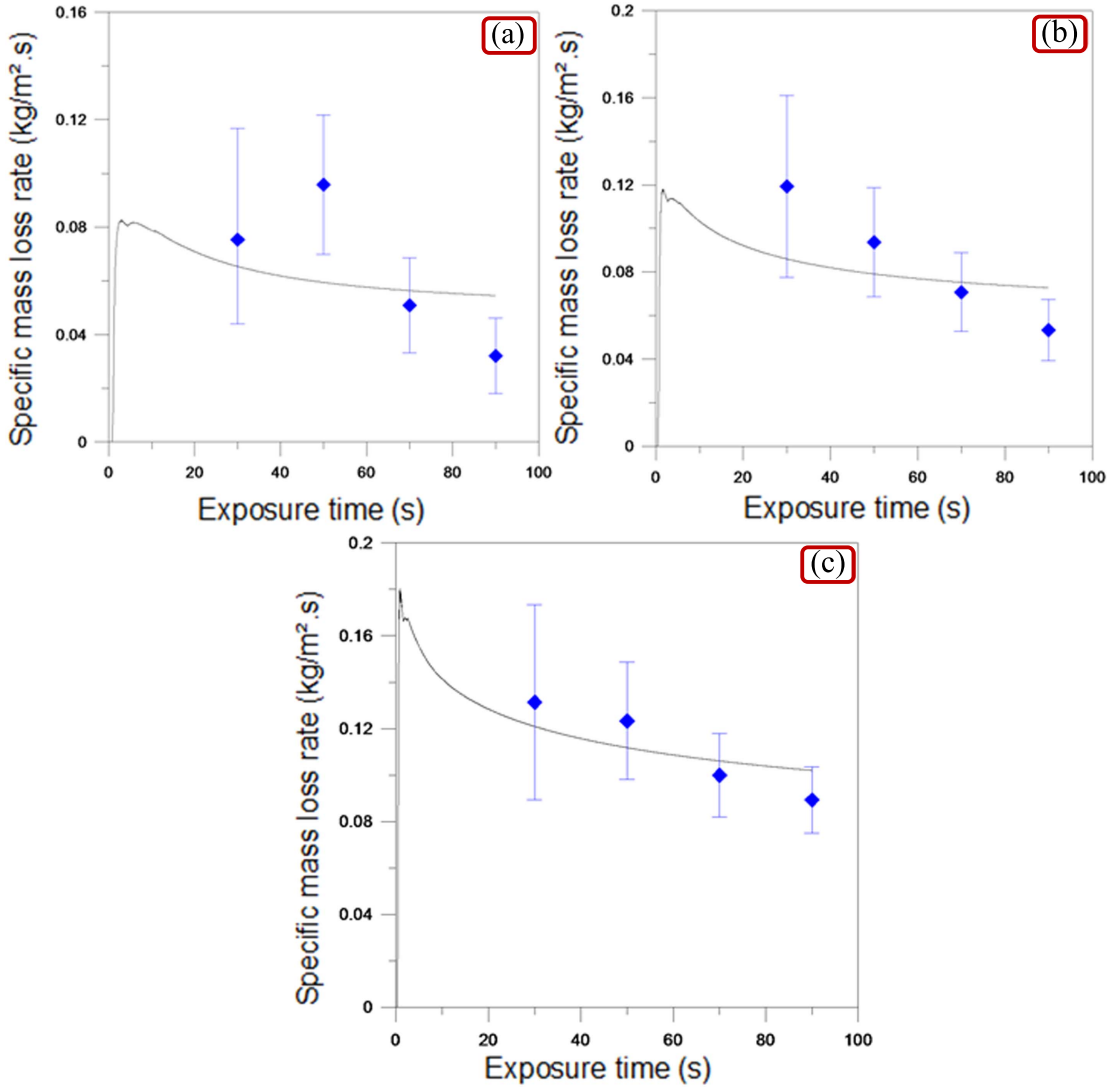

Figure 8. Specific mass loss rate simulation curves with the experimental results. (a) 0.626 MW m^{-2}; (b) 0.903 MW m^{-2} and (c) 1.379 MW m^{-2}.

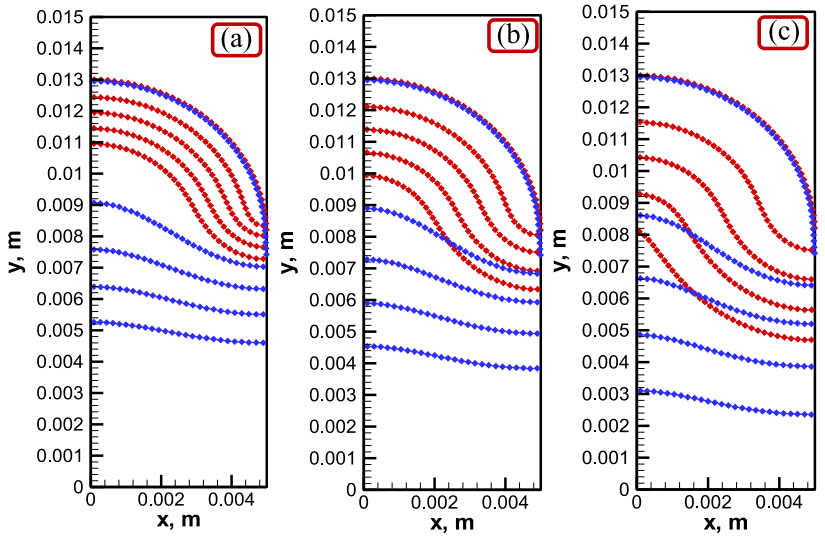

Figure 9. Interfaces evolution for 0 s, 30 s, 50 s, 70 s and 90 s of exposure: (a) 0.626 MW m^{-2}; (b) 0.903 MW m^{-2} and (c) 1.379 MW m^{-2}.

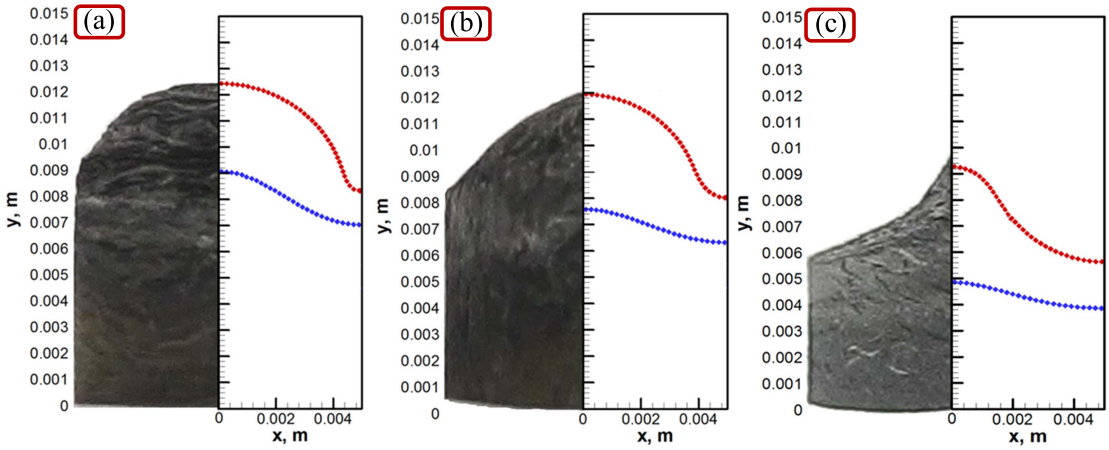

Figure 10. Interfaces evolution comparison to the cases of (a) 30 s in 0.626 MW m^{-2}; (b) 50 s in 0.626 MW m^{-2} and (c) 70 s in 1.379 MW m^{-2}.

Table 2. *rms* values of specific mass loss rate between tests and model.

Heat flux	*rms*
0.626 MW m^{-2}	0.4109
0.903 MW m^{-2}	0.2436
1.379 MW m^{-2}	0.0991
Total	0.3118

increase of the char layer on the surface reduces the pyrolysis velocity, since the heat flux does not reach the virgin material directly like it has on the beginning of the process.

Figure 8 shows the specific mass loss rate curves obtained from the computational simulation. In figure 8(a), the experimental result of 50 s is justified by an alignment error, which occurred in the samples tested in 0.626 MW m^{-2}, represented by the blue points. The other points are close to the simulation curve. The error bars are crossing the simulation line. In figures 8(b) and (c), the simulation results were close to the results obtained experimentally, hence, the error bars crossed the simulation curve too.

In figures 9 and 10, it is presented the interfaces evolution and some comparisons between the real profiles and those obtained from the computational simulation. The blue line shows the pyrolysis interface and the red one shows the char ablation interface.

Figure 10(a) presents a comparison for heat flux of 0.626 MW m^{-2} for 30 s. In figure 10(b), the comparison for the heat flux of 0.626 MW m^{-2} for 50 s and figure 10(c) shows a comparison for the heat flux of 1.379 MW m^{-2}. With these results, it is verified that the simulation of the interfaces evolution results in profiles which are very close to those obtained experimentally.

With the results of both the tests and the model, it was possible to obtain the *rms* (root mean square) value, which is the deviation of the specific mass loss rate results. This value is obtained from equations (4.1) and (4.2).

$$rms = \sqrt{\frac{\sum_{i=1}^{N} \Delta k_i^2}{N}} \tag{4.1}$$

$$\Delta k_i = \left(\frac{k_c - k_m}{k_m} \right) \times 100\% \tag{4.2}$$

Where k_c is the calculated value and k_m is the measured value. The *rms* values are shown to each heat flux tested on table 2.

The total deviation for the material of carbon/phenolic resulted in 0.3118 or 31.18%. Although this can be considered a high value, the graphics show that the simulation curves are within or very close to the error barrs in all heat fluxes and the real shape of surfaces after ablation are well represented by the numerical results in the cases selected, figure 10. Thus, the mathematical model is considered validated, proving effectiveness in its

purpose of predicting TPS material behavior in a real geometry, under these heat fluxes with acceptable accuracy.

5. Conclusion

Experimental procedures were implemented in the LPP Plasma Tunnel (ITA), as a heat flux curve as a function of the nozzle distance and implementation of mechanisms which made possible to run tests in lots of 8 samples, where the incidence surface and opposite surface temperatures were measured. These improvements support the development of qualification tools and certification of TPS materials for Brazilian aerospace industry.

The use of quartz/phenolic parts in the sample holder devices generates fluctuations in the measured temperature results in the thermocouple after lots of experiments. This can be avoided replacing this part to one made of a different material, which starts to ablate at a higher temperature.

The mass loss curves grow linearly with the time of exposure to the plasma jet. There is also an increase in the mass loss values with the increase of heat flux, which raises the temperature of the exposed surface. The results of specific mass loss rate shows that the higher the thermal flux, the higher the specific mass loss rate, but this value reduces with the time of exposure to the heat flux. It occurs due to the formation of char on the surface of the material, resulting from pyrolysis, creating a sort of thermal barrier.

After comparison among numerical and experimental results, the simulation model was considered validated, being effective in predicting TPS carbon/phenolic material behavior in a real geometry, under the tested heat fluxes because:

- When simulating the temperature of the back surfaces, the results obtained remain close to the simulation, taking into account dispersions and fluctuations generated by quartz/phenolic sample holder parts (CP 11);
- The model results of specific mass loss rate were close to the experimental results, the experimental error bars crossed the model curve, obtaining a *rms* value of 31.18%;
- The model results of pyrolysis and ablation interfaces evolution reached a great proximity to those experimentally obtained;

This work also raised new possibilities of research works, like the extension of the model's validation using the same experimental facility for other TPS materials, such as CRFC, Quartz/Phenolic, Carbon/Epoxy, which are already used in Brazilian aerospace vehicles, or others like AVCOAT, PICA, ASTERM and MonA, in different geometries.

ORCID iDs

Pedro Guilherme Silva Pesci https://orcid.org/0000-0002-8113-7230

References

[1] Da Costa L E V L 2003 The composite option for solid rocket motor cases in Brazil *Int. Astronautical Congress of The Int. Astronautical Federation, The Int. Academy of Astronautics, And the Int. Institute of Space Law, 54, 2003, Bremen, Proc.... (Reston)* (AIAA)
[2] Anderson J D Jr 1992 Aerothermodynamics: a tutorial discussion ed E A Thornton *Thermal Structures and Materials for High-Speed Flight* p 547(Washington: AIAA)
[3] Torre L, Kenny J M and Maffezzoli A M 2008 Degradation behavior of a composite material for thermal protection systems Part I-experimental characterization *Journal of Material Science* [S. l.] **33** 3137–43
[4] Silva S F C, Machado H A and Bittencourt E 2015 Effect of the fiber orientation relatively to the plasma flow direction in the ablation process of a carbon-phenolic composite. *Journal of Aerospace Technology and Management* São José dos Campos , **7** 43–52
[5] Barbosa C A L 2004 *Obtenção e Caracterização de Materiais Ablativos a Base de Compósitos de Fibra de Carbono/Resina Fenólica* p 142 (São José dos Campos: Instituto Tecnológico de Aeronáutica)
[6] Thimoteo H P C 1986 *Estudo do Comportamento Ablativo de Composições Fenólicas Com Carga* p 172(Rio de Janeiro: Universidade Federal do Rio de Janeiro)
[7] Paju J, Pehk T and Christjanson P 2009 Structure of phenol-formaldehyde polycondensates *Proc. of the Estonian Academy of Sciences* vol 58, pp 45–52
[8] Ghosh N N, Kiskan B and Yagci Y 2007 Polybenzoxazines—new high performance thermosetting resins: synthesis and properties *Prog. Polym. Sci.* [S. l.] **32** 1344–91
[9] Tran H K and Rasky D J 1994 Thermal response and ablation characteristics of lightweight ceramic ablators *Journal of Spacecraft and Rockets. Reston* **31** 993–8
[10] Tran H K, Johnson C E, Rasky D J, Hui F C L, Hsu M T and Chen Y K 1996 Phenolic impregnated carbon ablators (PICA) for discovery class missons *Thermophysics Conf., 31, 1996, New Orleans. Proc.*... p 14(Reston: AIAA)
[11] Ritter H, Bayle O, Mignot Y, Boulier E, Portela P, Bouilly J M and Sharda R 2011 Ongoing european developments on entry heatshields and TPS materials *Int. Planetary Probe Workshop, 8, 2011, Porstmouth. Proc.*... p 8

[12] Nguyen-Bui N T H, Duffa G, Dubroca B and Leroy B New methods for the simulation of ablative thermal protections *European Workshop of Thermal Protection Systems and Hot Structures, 5, 2006, Noordwijk. Proc.*... p 8
[13] Machado H A 2009 Two-dimensional simulation of multi-layer ablation-conduction problem in a rocket TPS via an interface tracking method *Thermophysics Conf. 41, 2009, San Antonio. Proc.*... p 13(Reston: AIAA)
[14] Auweter-Kurtz M, Kurtz H L and Laure S 1996 Plasma generators for re-entry simulation *Journal of Propulsion and Power, Reston* **12** 1053–61
[15] Regan F J and Anandakrishnan S M 1993 *Dynamics of Atmospheric Re-Entry* p 588(Washington: AIAA)
[16] Torre L, Kenny J M and Maffezzoli A M 1998 Degradation behavior of a composite material for thermal protection systems. Part II-process simulation *Journal of Material Science,* [S. l.] **33** 3145–9
[17] Charakhovski L *et al* 2008 *Hypersonic and Subsonic Plasma Setups for Testing Heat Shielding Materials Brazilian Congress of Thermal Engineering and Sciences, 12, 2008, Belo Horizonte. Proc.*... (Rio de Janeiro: ABCM)
[18] Williams S D and Curry D M 1992 Thermal protection materials—thermophysical property *Data (Nasa Reference Publication 1289)* p 234(Washington: NASA, dez)
[19] Sutton K 1970 *An Experimental Study of a Carbon-Phenolic Ablation Material (Nasa Technical Note TN D-5930)* p 51(Washington: NASA, set)
[20] Sykes G F 1967 Descomposition characteristics of a char-forming phenolic polymer used for ablative *Composites (Nasa Technical Note TN D-3810)* p 21(Washington: NASA, fev)